


# SCIENTIFIC REPORTS



OPEN

## High temperature tribology of polymer derived ceramic composite coatings

Sajid Ali Alvi & Farid Akhtar 

Polymer derived ceramic (PDC) composite coatings were deposited on AISI 304 substrates using siloxane based preceramic polymer polymethylsilsquioxane (PMS) and  $ZrSi_2$  as active filler or Ag as passive filler. The tribological performance of the composite coatings was evaluated at room temperature and moderately high temperatures (150 °C, 200 °C, 300 °C and 400 °C). The composite coatings showed low coefficient of friction (COF),  $\mu$ , from 0.08 to 0.2 for SiOC- $ZrSi_2$  composite coatings, and from 0.02 to 0.3 for SiOC-Ag composite coatings, at room temperature with increasing normal load from 1 to 5 N. High temperature tribology tests showed high COF values from 0.4 to 1 but low wear for SiOC- $ZrSi_2$  coating, and low COF from 0.2 to 0.3 for SiOC-Ag coatings at lower temperature ranges. Low load friction tests at room temperature showed negligible wear in SiOC- $ZrSi_2$  coatings, suggesting good wear resistant and lubricating properties due to formation of t- $ZrO_2$  and carbon. Low COF and high amount of wear was observed in SiOC-Ag composite coatings at room temperature due to high ductility of Ag and smearing of wear debris in the wear track. The coatings and wear tracks were characterized to evaluate the lubrication and wear behavior.

There is an ongoing demand for high temperature tribological coatings in different industries, such as coatings in aerospace (airfoil bearings, various satellite components and rolling element bearing) and automobile (engine bearings, piston assemble and traction drive), with tailored properties, such as high hardness, better friction and wear properties at higher temperatures, as well as oxidation and corrosion resistant properties<sup>1–3</sup>. In order to avoid the cost of designing new high temperature materials, it becomes economically viable to design a coating over conventional materials to sustain material damages at elevated temperatures.

Solid lubricants are utilized for high temperature application because of their low vapor pressure and sublimation. Solid lubricants for high temperature lubrication require good hardness, toughness, oxidation resistant, *in-situ* lubricating phases and high temperature stability<sup>4</sup>. Coatings for lubrication can be either intrinsic, facilitating interfacial shearing of atomic planes, or extrinsic, where additive from surrounding activates the shearing mechanism. However, most of the intrinsic or extrinsic coatings lose their lubricating properties above 300 °C. Therefore, Solid lubricants for higher temperature (>300 °C), such as soft metals (Ag, Cu, Au etc.), fluorides ( $CaF_2$ ,  $BaF_2$ ), and metal oxides ( $V_2O_5$ ,  $AgTiO_3$ ), combined with intrinsic or extrinsic solid lubricants, also known as chameleon coatings, can adapt to different temperature ranges of 25–1000 °C for giving lubricating properties<sup>5</sup>.

Various coating techniques have been explored to enhance the high temperature tribological properties. Laser clad coatings have been developed where coated material forms composite phases with substrate material. Different additives of  $WS_2/CaF_2/h$ -BN has been added to Ni alloy matrix powders and laser clad on Ti-6Al-4V substrate tested at different temperatures giving low COF of 0.32–0.35 (25 °C), 0.27–0.3 (300 °C) and 0.21–0.29 (600 °C) and wear rate was reduced to  $0.9–9 \times 10^{-5} \text{ mm}^3/\text{Nm}$  (25 °C),  $0.15–8 \times 10^{-5} \text{ mm}^3/\text{Nm}$  (300 °C) and  $2–4 \times 10^{-5} \text{ mm}^3/\text{Nm}$  (600 °C). The addition of additives formed phase, such as TiC,  $TiWC_2$ ,  $Ti_2CS$  and CrS (for  $WS_2$  addition);  $TiO_2$ , TiC and  $TiB_2$  (for h-BN addition), resulting in reduced wear rate and improved self-lubricating properties<sup>6–8</sup>. Magnetron sputtering has been explored to obtain thin composite/nanocomposite coatings of oxides and carbides for high temperature tribology. Coated and subsequent *in-situ* formed nanocomposite of yttria-stabilized zirconia (YSZ) coating containing Ag and Mo, and binary oxides of  $\alpha$ - $MoO_3$  and  $V_2O_5$  doped with Ag or Cu showed reduced COF from ~0.7 to 0.14 due to formation of magneli phases with increasing temperature up to 700 °C<sup>9–14</sup>. Ternary oxides of (Ag, Cu)-(Ta, W, Mo)-O have also been developed with magnetron sputtering to obtain good lubricating and wear properties at high temperatures, such as  $AgTaO_3$

Division of Materials Science, Luleå University of Technology, Luleå, 97187, Sweden. Correspondence and requests for materials should be addressed to S.A.A. (email: [sajid.alvi@ltu.se](mailto:sajid.alvi@ltu.se)) or F.A. (email: [farid.akhtar@ltu.se](mailto:farid.akhtar@ltu.se))

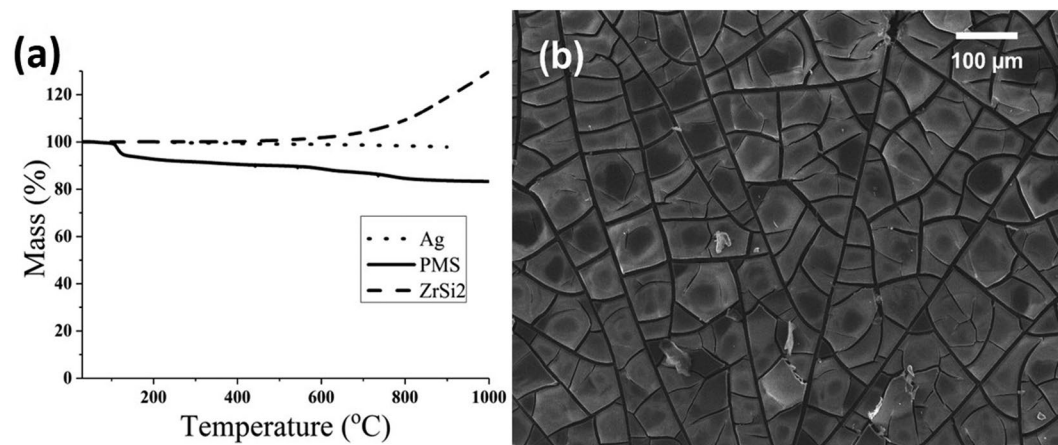


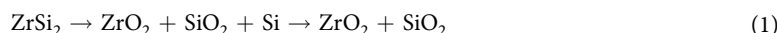
**Figure 1.** (a) TGA of PMS polymer precursor, Ag and ZrSi<sub>2</sub> powder, (b) PMS coating without filler after pyrolysis.

(750 °C; COF: 0.06; wear rate:  $4 \times 10^{-7}$  mm<sup>3</sup>/Nm), CuTa<sub>2</sub>O<sub>6</sub> (750 °C; COF: 0.24; wear rate:  $0.7 \times 10^{-7}$  mm<sup>3</sup>/Nm), Ag<sub>2</sub>Mo<sub>2</sub>O<sub>7</sub> (600 °C; COF: 0.12), and Ag<sub>2</sub>WO<sub>4</sub> (600 °C; COF: 0.43)<sup>15–17</sup>. Atomic layer deposition, with its ability to grow controlled coating layers, has been explored for high temperature tribology to develop nanocrystalline ZnO (room temperature (RT); COF: ~0.1), wear resistant nanolaminates of ZnO/Al<sub>2</sub>O<sub>3</sub>/ZrO<sub>2</sub> with a thickness of 140 nm (wear rate at 150 °C:  $3.6 \times 10^{-6}$  mm<sup>3</sup>/Nm; 400 °C:  $3.1 \times 10^{-5}$  mm<sup>3</sup>/Nm)<sup>18–20</sup>. Deposition methods, such as physical vapor deposition (PVD) and laser deposition, have been used to develop lubricious ZnO coatings (RT; COF: 0.1–0.2), wear resistant composite coatings of NiCrAlTi/TiC/Ti-CaF<sub>2</sub> (at 300 °C, wear rate:  $5 \times 10^{-5}$  mm<sup>3</sup>/Nm; and at 600 °C, wear rate:  $2 \times 10^{-5}$  mm<sup>3</sup>/Nm) and duplex treated nitride/TiAlN coatings (wear rate at 400 °C:  $7 \times 10^{-6}$  mm<sup>3</sup>/Nm, at 500 °C:  $4 \times 10^{-6}$  mm<sup>3</sup>/Nm, and at 600 °C:  $8 \times 10^{-6}$  mm<sup>3</sup>/Nm)<sup>21–23</sup>.

Ceramic coatings obtained from silicon-based polymer derived ceramics (PDCs) offer a simple, energy efficient robust technique to obtain coatings with tailored properties for larger and complex substrates. PDC coatings are obtained using organo-silicon precursors, such as polysiloxane<sup>24–27</sup>, polysilazane<sup>28–32</sup>, polycarbonylsilane<sup>33–35</sup> etc., to obtain SiOC, SiCN/Si<sub>3</sub>N<sub>4</sub>/SiOCN/SiC, and SiC coatings, respectively, after crosslinking and pyrolysis. The polymer-to-ceramic conversion is obtained at lower temperature of up to 800 °C, making it economical and environmentally effective compare to other coating techniques. The advantages of PDC coatings have been identified due to its inexpensive deposition techniques (such as dip coating, spin coating or spray coating), easier deposition with starting liquid phase, control over properties through nanostructure phases, and the ability to coat complex shapes<sup>36</sup>. The main drawback arises with PDC coating deposition from shrinkage during polymer to ceramic conversion, restricting coating thickness of pure PDC to only few microns. This problem has been overcome by using active or passive filler to compensate for the shrinkage arising from evaporation of volatile hydrocarbon and other compounds. Passive filler, such as BN, ZrO<sub>2</sub>, TiO<sub>2</sub> and SiC, can reduce the volume fraction of shrinkage phase, whereas active fillers, such Ti, Al, ZrSi<sub>2</sub>, TiSi<sub>2</sub> and TiB<sub>2</sub>, can react with gaseous products or atmosphere to form new phases<sup>37</sup>. Fillers may also modify the properties of coatings, such as thermal and electrical conductivity (such as graphite or ZrO<sub>2</sub>), thermal expansion (such as ZrO<sub>2</sub>), hardness (such as SiC and c-BN), and tribology (such as h-BN and c-BN). Recently, there have been few studies performed at room temperature and very low loads, in the range of mN, for lubricating behavior of coated/bulk PDCs<sup>38–42</sup>, and on composite PDC coatings with addition of h-BN and c-BN fillers<sup>43</sup>. However, there are no reports studying the tribological properties of PDC coatings at higher loads and temperatures to best of our knowledge. In this regards, the current work focuses on the design of PDC composite coatings that offer superior tribological properties at higher loads and temperatures. PDC composite coatings were designed using fillers, such as ZrSi<sub>2</sub> and Ag, which can give tribological properties at different temperatures.

## Results and Discussion

Thermal gravimetric analysis (TGA) of PMS polymer precursor in Fig. 1a shows three steps of ceramic conversion process giving ceramic yield of 83 wt.% on complete conversion to SiOC ceramic at 800 °C. According to previous reports on PMS conversion to ceramic, in the first step (110–370 °C) cross-linking occurs with the release of isopropanol and H<sub>2</sub>O; in the second step (460 to 670 °C) oligomers as well as ethanol evolve; and in the third step (650–1000 °C) conversion to SiOC completes with the release of H<sub>2</sub>, methane and trace amount of H<sub>2</sub>O<sup>44</sup>. Thermal behavior of ZrSi<sub>2</sub> showed a mass gain of 30 wt.% till 1000 °C. According to Gebwein *et al.*<sup>45</sup>, the mass gain of ZrSi<sub>2</sub> is related to oxidation, which starts at 500 °C and completes at 1000 °C with the formation of SiO<sub>2</sub> and ZrO<sub>2</sub> phases. They have suggested that ZrSi<sub>2</sub> oxidizes partially according to Wagner theory of selective oxidation<sup>46</sup>, where less noble element (Zr) is oxidized preferentially along with diffusion of Si atoms to bulk of material forming elemental silicon. In addition to this, non-preferential oxidation takes place up to 900 °C as shown in the reaction mechanism below:



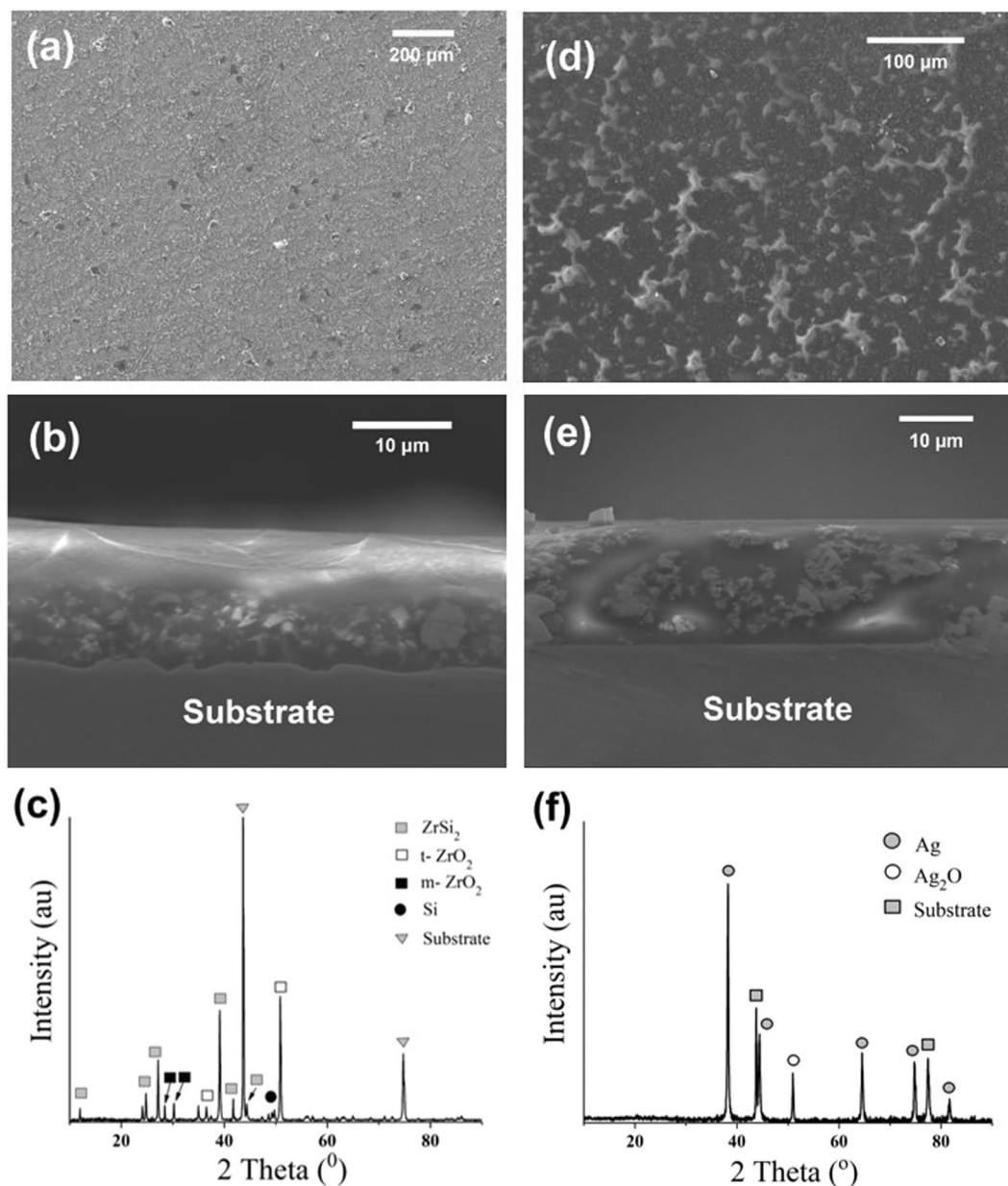


**Figure 2.** Characterization of SiOC-ZrSi<sub>2</sub> (a–c) and SiOC-Ag (d–f) coatings pyrolyzed at 700 °C. (a,d) SEM images of top surface, (b,e) SEM images of cross-section, (c,f) X-ray diffraction analysis.

Thermal behavior of Ag showed weight loss of 2 wt.% over the temperature range till 800 °C due to desorption of water. The mass loss of PMS during ceramic conversion process results in formation of cracks and delamination of coatings, as shown in Fig. 1b. This happens due to the severe increase in density and volume shrinkage on conversion to ceramic, thus limiting the PDC coating thickness without the aid of fillers<sup>47</sup>. In order to compensate for mass loss, 5 vol.% ZrSi<sub>2</sub> and Ag was added as a filler material to PMS to prepare films with less defects after pyrolysis.

Composite coatings (pyrolyzed at 800 °C, Ar atmosphere) showed relatively high amount of cracks and therefore were not analyzed further, see Supplement Information S1. The coatings pyrolyzed at 700 °C, with similar experimental conditions, showed crack-free microstructure and partial oxidation of fillers to form t-ZrO<sub>2</sub> and Ag<sub>2</sub>O phases, as seen in Fig. 2. The residual content of incomplete polymer was calculated to be around 5 wt% from TGA. The top view of the SiOC-ZrSi<sub>2</sub> coating (Fig. 2a) shows a uniform crack-free coating after pyrolysis. However, SiOC-Ag coating (Fig. 2d) shows presence of aggregates on the surface. Such aggregates form in SiOC-Ag coatings due to its addition to polymeric solution with high viscosity. The aggregation of Ag nanoparticles has been attributed to the attractive forces created by van der Waals forces or chemical bonds between nanoparticles<sup>48</sup>. Whilst, ZrSi<sub>2</sub> act as an active filler and counters the formation of cracks and aggregation in SiOC-ZrSi<sub>2</sub> coatings<sup>49,50</sup>. The cross-section of the composite coatings revealed a uniform coating thickness of ~12 μm, Fig. 2(b,e), where ZrSi<sub>2</sub> is distributed uniformly and Ag is aggregated, which tends to happen during its mixing with polymeric precursor. Microhardness of SiOC-ZrSi<sub>2</sub> coating was found to be 200 Hv, as shown

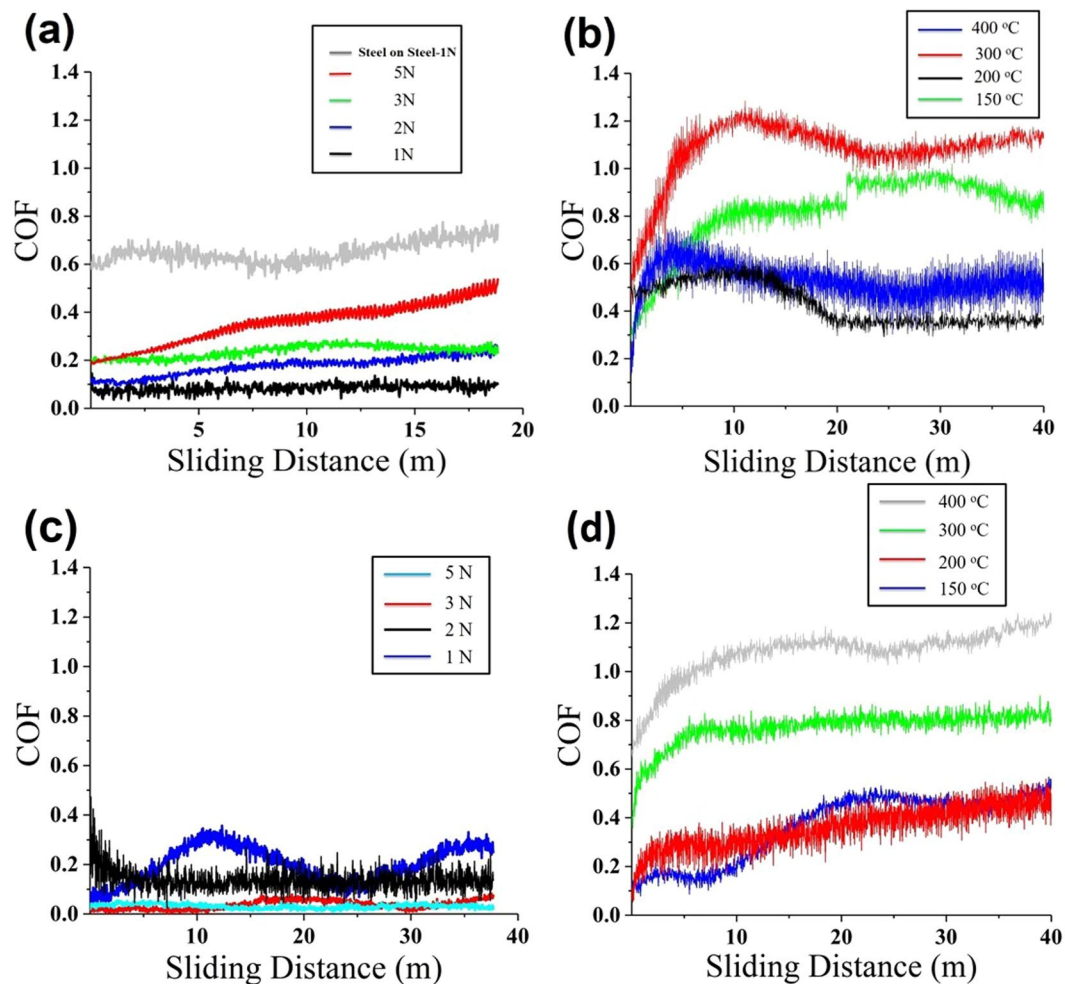
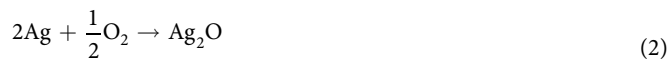


**Figure 3.** Friction coefficient curves of SiOC-ZrSi<sub>2</sub> and SiOC-Ag composite coating: (a) SiOC-ZrSi<sub>2</sub> at room temperature with various loads, and (b) SiOC-ZrSi<sub>2</sub> at higher temperatures with 1 N load; (c) SiOC-Ag at room temperature with various loads, and (d) SiOC-Ag at higher temperatures with 1 N load.

in Fig. S11. The optical profilometry of SiOC-ZrSi<sub>2</sub> composite coating showed that the coating surface had a surface roughness of 800 nm, as shown in Supplementary Information S2. The X-ray diffraction (XRD) data of SiOC-ZrSi<sub>2</sub> coating show phases of ZrSi<sub>2</sub>, SiO<sub>2</sub> and tetragonal-ZrO<sub>2</sub> (t-ZrO<sub>2</sub>) (Fig. 2c); while of SiOC-Ag coatings show presence of Ag and Ag<sub>2</sub>O (Fig. 2f).

The oxidation of Ag to Ag<sub>2</sub>O has been studied by X. Bao *et al.*<sup>51</sup> at higher temperatures, showing the formation of Ag<sub>2</sub>O using x-ray photoelectron spectroscopy (XPS), where the binding energy and O/Ag ratio changes from 530 eV and 0.2 at 300 °C to 529 eV and 0.5 at 600 °C, respectively, which corresponds to formation of stoichiometric Ag<sub>2</sub>O. The oxidation reaction of Ag nanoparticles takes place by:



Although, the complete ceramization of PMS preceramic polymer takes place at 800 °C, the coating was pyrolyzed at 700 °C to combine the properties of ceramic coating with incomplete precursor conversion to enhance lubricating properties. Formation of sp<sup>2</sup> carbon has been reported during the polymer-to-ceramic conversion of PDC, which can be particularly advantageous to the lubricating properties<sup>52</sup>. Furthermore, t-ZrO<sub>2</sub> and SiO<sub>2</sub> phases observed arise from the partial oxidation of ZrSi<sub>2</sub>, which has been reported to be beneficial towards load bearing capability<sup>53</sup>.

The energy dispersive x-ray spectroscopy (EDS) mapping of SiOC-ZrSi<sub>2</sub> and SiOC-Ag coating cross-section is shown in supplementary information, Fig. S3. High amount of elemental zirconium can be observed at lower section of coating as ZrSi<sub>2</sub> with 2–3 μm particle sizes are placed near the substrate, and top coating mostly consists of Si, O and C. The formation of Ag aggregates in SiOC-Ag coating is evident in EDS mapping.

The friction coefficient versus the sliding distance curves of SiOC-ZrSi<sub>2</sub> and SiOC-Ag coatings with varying loads and at various temperatures are shown in Fig. 3. Steel ball on steel substrate friction test at 1 N normal load showed an average COF of 0.66, as shown in Fig. 3a. The wear track of steel-on-steel showed high amount of abrasive and adhesive wear along with high amount of transfer layer on steel counter ball, as shown in Fig. S9a,b,

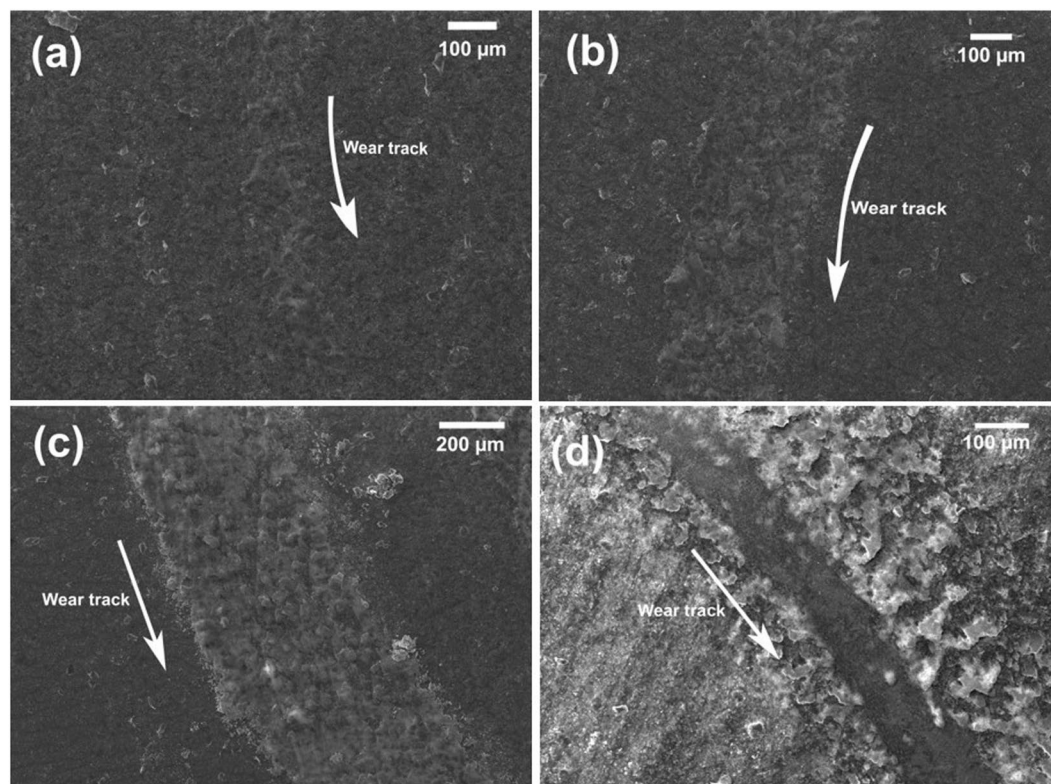


**Figure 4.** SEM image of wear tracks from SiOC-ZrSi<sub>2</sub> at room temperature with a sliding distance of 18 m at (a) 1 N load; (b) 2 N load; (c) 3 N load; and (d) 5 N load.

respectively. SiOC-ZrSi<sub>2</sub> composite coating, at room temperature with 1 N load, shows the lowest COF of 0.08, which increases with increasing load from 1 N to 5 N from 0.08 to 0.5, as shown in Fig. 3a. It has been reported in the literature that the polymer derived SiOC containing high amount of carbon with sp<sup>2</sup> structure can act as self-lubricant layer by formation of a thin transfer layer on the ball surface<sup>39,54</sup>. Furthermore, the presence of t-ZrO<sub>2</sub> and SiO<sub>2</sub> (Fig. 2e) may enhance the load bearing properties<sup>45,53</sup>. The friction test performed at a higher load of 5 N shows that the coating was intact after 20 m sliding distance. The COF increased to 0.5, however it was lower than the steel-to-steel friction coefficient of 0.66. The low COF and stability of the coating is attributed to the formation of sp<sup>2</sup> carbon, as determined by XRD after polymer to ceramic conversion<sup>52</sup> and elemental Si (Fig. 2c) and incomplete (5 wt% retained polymer, as determined by TGA) conversion of polymeric precursor.

The morphology of wear tracks and counter steel ball after friction tests on SiOC-ZrSi<sub>2</sub> coatings at room temperature at various loads can be seen in Fig. 4(a–d) and in supplementary information Fig. S4, respectively. Wear tracks after friction tests at 1 N, 2 N and 3 N load (Fig. 4a–c) and corresponding EDS (Fig. S5) showed that there was less wear of the coating with low amount of iron (Fe) present in the wear track. On increasing load to 5 N, extensive wear of the coating is visible (Fig. 4d). The corresponding EDS (Fig. 5S, site 4) confirms the presence of coating after the test. The scratch test showed an adhesion of 6 N, as shown in Fig. S10, after which an abrupt increase in COF was caused by coating failure. This suggests good adhesion of coating to the substrate even with wear at higher load. The strong adhesion is attributed to the direct chemical bonding between the substrate and polymeric precursor as PMS reacts with hydroxyl groups present at the steel surface, forming metal-O-Si bonds<sup>55</sup>. The microstructure and EDS analysis of steel counter balls show negligible coating transfer after friction tests at lower load, as shown in S4.

Friction curves (Fig. 3c) and corresponding wear tracks (Fig. 5a–d) summarize the performance of SiOC-Ag composite coatings at room temperature and various loads. The friction test at 1 N showed a varying COF between 0.08 and 0.3, which could be related to the slipping and gripping of counter ball with Ag and SiOC. The average COF decreased to 0.15, 0.04 and 0.02 at loads of 2 N, 3 N and 5 N, respectively. The very low COF values are related to smearing effect of Ag in the coating and lubrication through transfer of coating to counter balls. Lubrication through coating transfer is observed on the counter ball, where the amount of transferred coating increased with increasing loads, as shown in supplementary information Fig. S8 and corresponding EDS analysis in Table S8. The wear track resulting from 1 N load, Fig. 5a, shows low amount of wear; whereas, coating removal is observed at higher loads in addition to smearing of Ag in the wear tracks, as shown in Fig. 5b–d. In contrast to friction properties of SiOC-ZrSi<sub>2</sub> coatings, SiOC-Ag has lower load bearing capability.

High temperature friction tests and corresponding wear tracks of SiOC-ZrSi<sub>2</sub> coatings are shown in Fig. 3b and Fig. 6(a–d), respectively. It can be seen that friction tests at 150 °C and 300 °C show higher COF values of 0.9 and 1.1, respectively, which are higher than COF of steel of 0.6–0.8. On increasing the temperature to 200 °C and 400 °C, the COF reduces to 0.4 and 0.45 after initial high COF due to run-in period, as shown in Fig. 3b. The

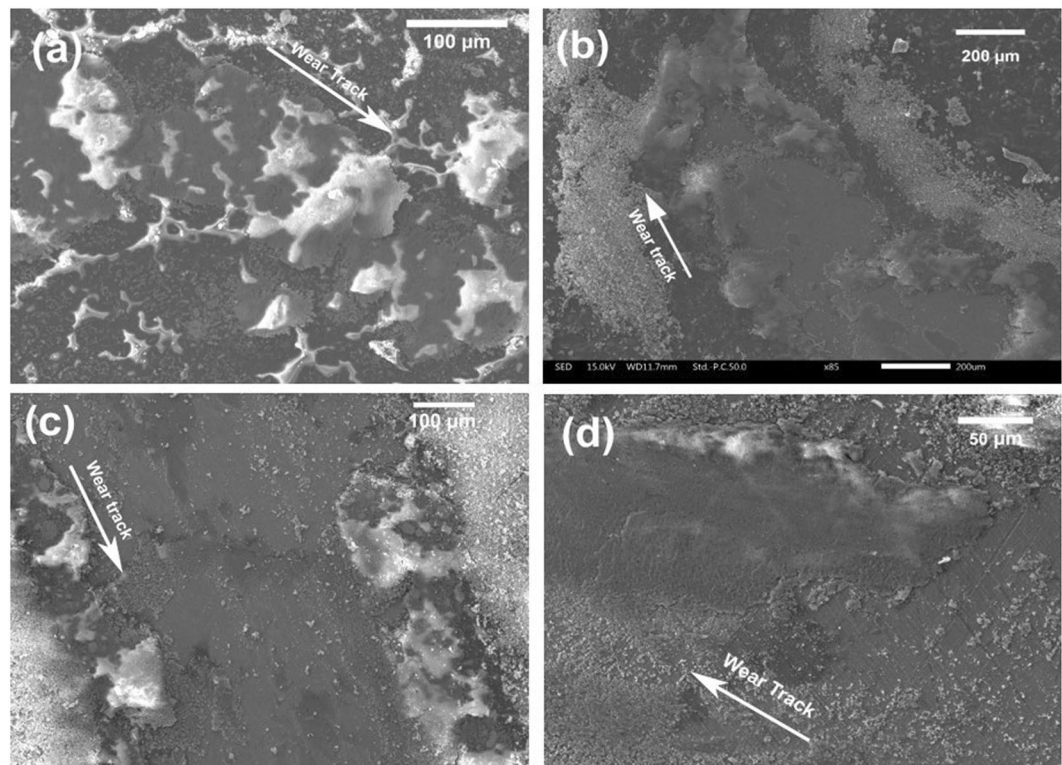


**Figure 5.** SEM micrographs of wear tracks of SiOC-Ag composite coating: (a) 1 N load; (b) 2 N load, (c) 3 N load; and (d) 5 N load.

subsequent reduction in friction can be related to transferred coating lubrication, which consequently reduces the friction between counter steel ball and coated substrate<sup>56</sup>. The wear tracks of the corresponding high temperature friction test showed low wear where coating was not completely removed, as shown in Fig. 6(a–d). It can be observed from EDS analysis of the wear track, as shown in Fig. S6, that the coating was sheared over the wear track during all friction tests, which can be related to the softening of unconverted polymeric phase in the coatings at higher temperature. The EDS analyses of the wear tracks show the presence of high amount of Si, O, and Zr and small amount of Fe over wear tracks (S6), suggesting that coating wasn't removed during the test. The coating transfer layers analyzed with EDS analysis on the counter steel ball after high temperature friction tests showed that the amount of transfer layers increased with increasing test temperatures and subsequently shielding the ball surface from contact with specimen surface to give low friction and wear, as shown in S7. The highest amount of transferred coating material was observed during 400 °C friction test, which resulted in reduced COF compare to other temperature tests.

Similarly, high temperature friction tests were performed at SiOC-Ag composite coatings at temperatures of 150 °C, 200 °C, 300 °C, and 400 °C, as shown in Fig. 3d. In contrast to high temperature friction tests over SiOC-ZrSi<sub>2</sub> coatings, SiOC-Ag composite coatings showed low average COF in the range of 0.2 to 0.5 at lower temperature of 150 °C and 200 °C, and coating transfer was observed after 1–2 m of initial sliding. The wear tracks corresponding to high temperature friction tests showed high wear, delamination of coatings at different places along with smearing of Ag in the wear track as well as in the delaminated coating regions, as shown in Fig. 6(e–h).

The high temperature tribology tests of PDC composite coatings suggest that the use of active filler ZrSi<sub>2</sub> enhances the load bearing and lubricating properties of coatings up to 4 N normal loads. Whereas, addition of passive filler, Ag nanoparticles, enhances the lubricating properties through transfer coating lubrication at room temperature as well as high temperature friction but limits the applied load to 1 N.

In conclusion, two types of ceramic filler/PDC composite coating were developed in this work using spin coating to enhance the tribological properties at room temperature and to some extent at high temperature (400 °C). PDC composite coatings of SiOC-ZrSi<sub>2</sub> and SiOC-Ag with a thickness of ~12 μm was obtained using spin coating. SiOC-ZrSi<sub>2</sub> showed low COF from 0.08 to 0.3 with increasing load from 1 to 5 N load. High temperature friction test on SiOC-ZrSi<sub>2</sub> showed a decreasing trend in COF with increasing temperature to 400 °C. Such high load bearing in SiOC-ZrSi<sub>2</sub> has been suggested due to the formation of t-ZrO<sub>2</sub> from partial oxidation of active-filler ZrSi<sub>2</sub>, formation of sp<sup>2</sup> carbon network and partial conversion of polymer to ceramic. The friction tests on SiOC-Ag coatings revealed decreasing average COF values from 0.2 to 0.02 with increasing loads at room temperature from 1 to 5 N. The low COF in SiOC-Ag composite coatings arises due to Ag lubricating properties and smearing effect of Ag wear debris in the wear track. The high temperature friction tests of SiOC-Ag composite coating showed low COF in the range of 150–200 °C over constant low load due to low shear strength of Ag. However, the tribological property of Ag becomes poor due to excessive softening at 300 °C.

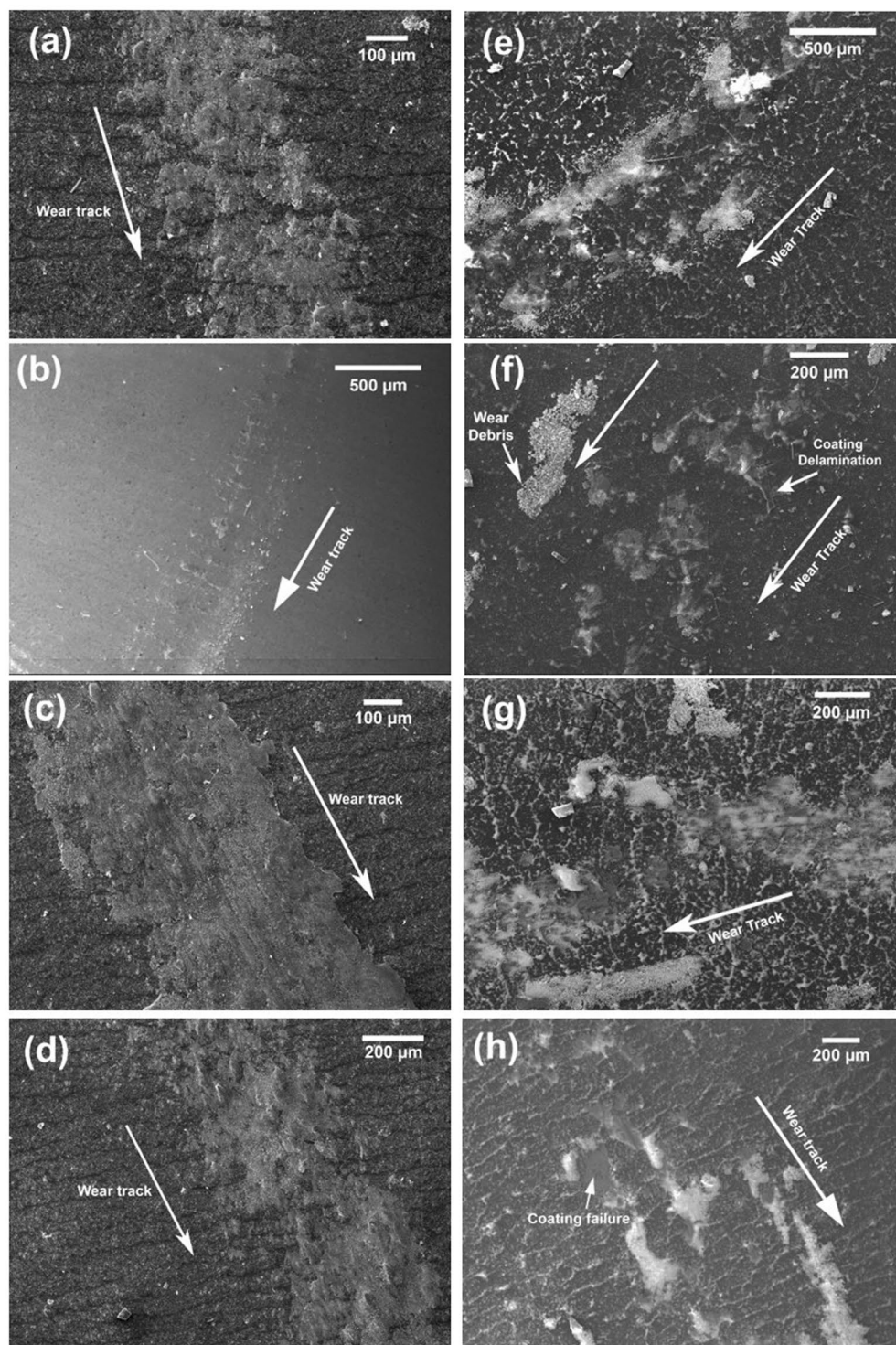


**Figure 6.** SEM images of wear tracks of SiOC-ZrSi<sub>2</sub> composite coatings with 1 N load at different temperatures for: (a) 150 °C, (b) 200 °C, and (c) 300 °C, (d) 400 °C; and SiOC-Ag composite coatings: (e) 150 °C; (f) 200 °C; (g) 300 °C, (h) 400 °C.

## Methods

**Coating Deposition.** Coatings of SiOC-ZrSi<sub>2</sub> and SiOC-Ag investigated in this work were developed using commercially available polymeric precursor polymethylsilsequioxane (PMS, MK Belsil, PMS, Wacker, GmbH, Germany), zirconium disilicide (3 μm, US Research Nanomaterials Inc., USA) as active filler material, and silver (70–80 nm, US Research Nanomaterial Inc., USA) as passive filler material. Polymeric suspension was developed using PMS (23 vol%), isopropanol (72 vol%, IPA), ZrSi<sub>2</sub> and Ag (5 vol%). PMS precursor was first dissolved in IPA with magnetic stirrer, followed by addition of Ag or ZrSi<sub>2</sub> and further mixing. The resulting suspensions were

ball-milled for 1 hour (ZrSi<sub>2</sub> filler) and 24 hours (Ag filler) to homogenize the mixture. AISI 304 stainless steel sheets was used as a substrate material. The substrate sheets were polishing with SiC papers to achieve surface roughness of 1 μm for better adhesion, followed by cleaning with ethanol in sonicator and drying in oven at 120 °C for 2 hour. Polymeric suspension was deposited on steel substrate using spin coater at 1000 rpm for 10 seconds. The resulting coatings were cross-linked at 190 °C for 1 hr in air using Nabertherm box furnace, followed by pyrolysis at 700 °C for 1 hr in argon atmosphere using Nabertherm tube furnace to convert PMS preceramic polymer to SiOC ceramic.

**Coating Characterization.** The coating microstructure and elemental composition were characterized using scanning electron microscopy (SEM, JSM-IT300LV, JEOL GmbH, Germany) and energy dispersive x-ray spectroscopy (EDS) using working distance of 10 mm and accelerating voltage of 15 kV. For EDS analysis of wear tracks, low accelerating voltage of 10 kV was used to lower the interaction volume on the surface and area analysis of around 200 × 200 μm was used. EDS area analysis was performed at 6 different places around each wear track. Thermal behavior of pre-ceramic polymer, ZrSi<sub>2</sub>, and Ag was analyzed till 1000 °C with a heating rate of 10 °C/min in air atmosphere using thermogravimetric analyzer (TGA 8000, Perkin Elmer, USA). The phases in coating were identified using Cu Kα radiation X-ray diffraction with monochromator (PANalytical Empyrean). Microhardness of coating was measured using Vickers microhardness. The surface of coating was analyzed using optical profiler (Wyko 1100 3D) by considering the Ra parameter of the coating.

**Tribological Characterization.** Friction tests were performed in air atmosphere with relative humidity of 50% using steel ball-on-disc modular-tribometer (Rtec Universal Tribometer, San Jose, USA) at room temperature (22 °C) and high temperatures (150 °C, 200 °C, 300 °C, and 400 °C). AISI 304 stainless steel substrate with a dimension of 15 mm × 15 mm was used for room temperature tests and a circular disc with 50.8 mm diameter for high temperature tests. Counter ball of E52100 alloy steel (Grade 25) with a hardness 60–66 HRC; and diameter of 6.5 and 9.5 mm for room temperature and high temperature friction tests, respectively, were used. The normal load was varied from 1 to 5 N, corresponding to maximum hertzian contact pressure of 448 to 767 MPa for steel ball on steel substrate, and a constant speed of 100 rpm and 50 rpm was applied for 10 minutes timespan for room temperature and high temperature tests, respectively. The friction tests were repeated with at least 4 coatings of each composition to obtain repeatability and their statistics are stated in Table S12. These experimental conditions have been chosen for applications, such as MEMS, where low load (mN) is applied.

## References

- Baker, C. C., Chromik, R. R., Wahl, K. J., Hu, J. J. & Voevodin, A. A. Preparation of chameleon coatings for space and ambient environments. *Thin Solid Films* **515**, 6737–6743 (2007).
- Erdemir, A. Review of engineered tribological interfaces for improved boundary lubrication. *Tribol. Int.* **38**, 249–256 (2005).
- Tung, S. C. & McMillan, M. L. Automotive tribology overview of current advances and challenges for the future. *Tribol. Int.* **37**, 517–536 (2004).
- Voevodin, A. A. & Zabinski, J. S. Nanocomposite and nanostructured tribological materials for space applications. *Compos. Sci. Technol.* **65**, 741–748 (2005).
- Prasad, T. W. S. V. Solid lubricants: a review. 511–531, <https://doi.org/10.1007/s10853-012-7038-2> (2013).
- Liu, X.-B. *et al.* A comparative study of laser cladding high temperature wear-resistant composite coating with the addition of self-lubricating WS<sub>2</sub> and WS<sub>2</sub>(Ni-P) encapsulation. *J. Mater. Process. Technol.* **213**, 51–58 (2013).
- Xiang, Z. F. *et al.* Investigation of laser cladding high temperature anti-wear composite coatings on Ti6Al4V alloy with the addition of self-lubricant CaF<sub>2</sub>. *Appl. Surf. Sci.* **313**, 243–250 (2014).
- Lu, X. L. *et al.* Synthesis and characterization of Ni60-hBN high temperature self-lubricating anti-wear composite coatings on Ti6Al4V alloy by laser cladding. *Opt. Laser Technol.* **78**, 87–94 (2016).
- Gulbiński, W., Suszko, T., Sienicki, W. & Warcholiński, B. Tribological properties of silver- and copper-doped transition metal oxide coatings. *Wear* **254**, 129–135 (2003).
- Gulbiński, W. & Suszko, T. Thin films of MoO<sub>3</sub>-Ag<sub>2</sub>O binary oxides – the high temperature lubricants. *Wear* **261**, 867–873 (2006).
- Fateh, N., Fontalvo, G. A., Gassner, G. & Mitterer, C. Influence of high-temperature oxide formation on the tribological behaviour of TiN and VN coatings. *Wear* **262**, 1152–1158 (2007).
- Fateh, N., Fontalvo, G. A. & Mitterer, C. Tribological properties of reactive magnetron sputtered V<sub>2</sub>O<sub>5</sub> and VN-V<sub>2</sub>O<sub>5</sub> coatings. *Tribol. Lett.* **30**, 21–26 (2008).
- Mu, Y., Liu, M., Wang, Y. & Liu, E. PVD multilayer VN-VN/Ag composite coating with adaptive lubricious behavior from 25 to 700 °C. *RSC Adv.* **6**, 53043–53053 (2016).
- Muratore, C., Voevodin, A. A., Hu, J. J. & Zabinski, J. S. Tribology of adaptive nanocomposite yttria-stabilized zirconia coatings containing silver and molybdenum from 25 to 700 °C. *Wear* **261**, 797–805 (2006).
- Stone, D. *et al.* Layered atomic structures of double oxides for low shear strength at high temperatures. *Scr. Mater.* **62**, 735–738 (2010).
- Stone, D. S. *et al.* Lubricious silver tantalate films for extreme temperature applications. *Surf. Coatings Technol.* **217**, 140–146 (2013).
- Gao, H. *et al.* (Ag, Cu)-Ta-O Ternaries As High-Temperature Solid-Lubricant Coatings. *ACS Appl. Mater. Interfaces* **7**, 15422–15429 (2015).
- Zhimin, C., Xinchun, L. & Dannong, H. Atomic layer deposition of zinc oxide films: Effects of nanocrystalline characteristics on tribological performance. *Surf. Coatings Technol.* **207**, 361–366 (2012).
- Mohseni, H. & Scharf, T. W. Atomic layer deposition of ZnO/Al<sub>2</sub>O<sub>3</sub>/ZrO<sub>2</sub> nanolaminates for improved thermal and wear resistance in carbon-carbon composites. *J. Vac. Sci. Technol. a-Vacuum Sci.* **149** (2015).
- Mohseni, H. & Scharf, T. W. Role of atomic layer deposited solid lubricants in the sliding wear reduction of carbon – carbon composites at room and higher temperatures. **333**, 1303–1313 (2015).
- Zabinski, J. S. Lubricious zinc oxide films: synthesis, characterization and tribological behaviour. *J. Mater. Sci.* **32**, 5313–5319 (1997).
- Luo, J. *et al.* Synthesis of High-Temperature Self-lubricating Wear Resistant Composite Coating on Ti6Al4V Alloy by Laser Deposition. *J. Mater. Eng. Perform.* **24**, 1881–1889 (2015).
- Niu, R., Li, J., Wang, Y., Chen, J. & Xue, Q. Structure and high temperature tribological behavior of TiAlN/nitride duplex treated coatings on Ti6Al4V. *Surf. Coatings Technol.* **309**, 232–241 (2017).
- Kendrick, T. C., Parbhoo, B. & White, J. W. Siloxane Polymers and Copolymers. In *Organic Silicon Compounds* (1989) 1289–1361, <https://doi.org/10.1002/0470025107.ch21> (John Wiley & Sons, Ltd, 2004).



25. Arkles, B. C. Polysilane-Siloxane Oligomers and Copolymer and Methods of Making the Same. *U.S. Pat. 4,626,583 assigned to Petrarc. Syst. Inc* (1986).
26. Blum, Y. D., MacQueen, D. B. & Kleebe, H.-J. Synthesis and characterization of carbon-enriched silicon oxycarbides. *J. Eur. Ceram. Soc.* **25**, 143–149 (2005).
27. Soraru, G. D., D'Andrea, G., Campostrini, R., Babonneau, F. & Mariotto, G. Structural Characterization and High-Temperature Behavior of Silicon Oxycarbide Glasses Prepared from Sol-Gel Precursors Containing Si-H Bonds. *J. Am. Ceram. Soc.* **78**, 379–387 (1995).
28. Kruger, C. R. & Rochow, E. G. Polyorganosilazanes. *J. Polym. Sci. Part A 2*, 3179–3189 (1964).
29. Blum, Y. D., Schwartz, K. B. & Laine, R. M. Preceramic polymer pyrolysis - Part 1 Pyrolytic properties of polysilazanes. *J. Mater. Sci.* **24**, 1707–1718 (1989).
30. Lavedrine, A. *et al.* Pyrolysis of polyvinylsilazane precursors to silicon carbonitride. *J. Eur. Ceram. Soc.* **8**, 221–227 (1991).
31. Horz, M. *et al.* Novel polysilazanes as precursors for silicon nitride/silicon carbide composites without 'free'carbon. *J. Eur. Ceram. Soc.* **25**, 99–110 (2005).
32. Vakifahmetoglu, C. *et al.* Highly porous macro- and micro-cellular ceramics from a polysilazane precursor. *Ceram. Int.* **35**, 3281–3290 (2009).
33. Shiina, K. & Kumada, M. Thermal Rearrangement of Hexamethyldi- silane to Trimethyl(dimethylsilylmethyl)- silane. *Org. Chem.* **23**, 139–139 (1958).
34. Schilling, C. L., Wesson, J. P. & Williams, T. C. Polycarbosilane Precursors for Silicon Carbide. *Am. Ceram. Soc. Bull.* **62**, 912–915 (1983).
35. Whitmarsh, C. K. & Interrante, L. V. Synthesis and Structure of a Highly Branched Polycarbosilane Derived from (Chloromethyl) trichlorosilane. *Organochemicals* **10**, 1336–1344 (1991).
36. Colombo, P., Mera, G., Riedel, R. & Sorar, G. D. Polymer-derived ceramics: 40 Years of research and innovation in advanced ceramics. *J. Am. Ceram. Soc.* **93**, 1805–1837 (2010).
37. Greil, P. Advancements in polymer-filler derived ceramics. *J. Korean Ceram. Soc.* **49**, 279–286 (2012).
38. Crosst, T. J., Raj, R., Cross, T. J., Prasad, S. V. & Tallant, D. R. Synthesis and Tribological Behavior of Silicon Oxycarbide Thin Films Derived from Poly(Urea)Methyl Vinyl Silazane, <https://doi.org/10.1002/9780470588246.ch32>.
39. Klaffke, D., Wäsche, R., Janakiraman, N. & Aldinger, F. Tribological characterisation of siliconcarbonitride ceramics derived from preceramic polymers. *Wear* **260**, 711–719 (2006).
40. Cross, T., Raj, R., Prasad, S. V., Buchheit, T. E. & Tallant, D. R. Mechanical and Tribological Behavior of Polymer-Derived Ceramics Constituted from SiC<sub>x</sub>O<sub>y</sub>N<sub>z</sub>. *J. Am. Ceram. Soc.* **89**, 3706–3714 (2006).
41. Bakumov, V. *et al.* Mechanical and tribological properties of polymer-derived Si/C/N sub-millimetre thick miniaturized components fabricated by direct casting. *J. Eur. Ceram. Soc.* <https://doi.org/10.1016/j.jeurceramsoc.2012.01.007> (2012).
42. Bongio, E. V., Lewis, S. L., Welson, D. R. & Sherwood, W. J. Polymer derived ceramic matrix composites for friction applications. *Adv. Appl. Ceram.* **108**, 483–487 (2009).
43. Barroso, G., Kraus, T., Degenhardt, U., Scheffler, M. & Motz, G. Functional Coatings Based on Preceramic Polymers\*\*, <https://doi.org/10.1002/adem.201500600>.
44. Ionescu, E. *et al.* Polymer-derived silicon oxycarbide/hafnia ceramic nanocomposites. Part I: Phase and microstructure evolution during the ceramization process. *J. Am. Ceram. Soc.* <https://doi.org/10.1111/j.1551-2916.2010.03765.x>.
45. Gefßwein, H., Pfrengle, A., Binder, J. R. & Haußelt, J. Kinetic model of the oxidation of ZrSi<sub>2</sub> powders. *J. Therm. Anal. Calorim.* **91**, 517–523 (2008).
46. Wagner, C. Formation of Composite Scales Consisting of Oxides of Different Metals. *J. Electrochem. Soc.* **103**, 627–633 (1956).
47. Goerke, O., Feike, E., Heine, T., Trampert, A. & Schubert, H. Ceramic coatings processed by spraying of siloxane precursors (polymer-spraying). *J. Eur. Ceram. Soc.* **24**, 2141–2147 (2004).
48. Zare, Y. Study of nanoparticles aggregation/agglomeration in polymer particulate nanocomposites by mechanical properties. *Compos. Part A Appl. Sci. Manuf.* **84**, 158–164 (2016).
49. Nguyen, M. D. *et al.* Novel polymer-derived ceramic environmental barrier coating system for carbon steel in oxidizing environments. *J. Eur. Ceram. Soc.* <https://doi.org/10.1016/j.jeurceramsoc.2016.12.049> (2017).
50. Greil, P. Active-Filler-Controlled Pyrolysis of Preceramic Polymers. *J. Am. Ceram. Soc.* **78**(4), 835–845 (1995).
51. Bao, X., Muhler, M., Schedel-Niedrig, T. & Schlögl, R. Interaction of oxygen with silver at high temperature and atmospheric pressure: A spectroscopic and structural analysis of a strongly bound surface species. *Phys. Rev. B - Condens. Matter Mater. Phys.* **54**, 2249–2262 (1996).
52. Ionescu, E. *et al.* Polymer-derived SiOC/ZrO<sub>2</sub> ceramic nanocomposites with excellent high-temperature stability. *J. Am. Ceram. Soc.* **93**, 241–250 (2010).
53. Chen, H., Zhang, Y. & Ding, C. Tribological properties of nanostructured zirconia coatings deposited by plasma spraying. **253**, 885–893 (2002).
54. Hirvonen, J. P. *et al.* Tribological characteristics of diamond-like films deposited with an arc-discharge method. *J. Mater. Res.* **5**, 2524–2530 (1990).
55. Günthner, M. *et al.* Advanced coatings on the basis of Si(C)N precursors for protection of steel against oxidation. *J. Eur. Ceram. Soc.* **29**, 2061–2068 (2009).
56. Chapter 4 Tribological Properties of Coatings. *Tribol. Ser.* **28**, 125–256 (1994).

## Acknowledgements

This work was supported by the Swedish Foundation for Strategic Research (SSF) for Infrastructure Fellowship Grant No. RIF14–0083.

## Author Contributions

Farid Akhtar and Sajid Ali Alvi conceived as well as conducted the experiments. All authors participated in analysing the results and reviewing the manuscript.

## Additional Information

**Supplementary information** accompanies this paper at <https://doi.org/10.1038/s41598-018-33441-8>.

**Competing Interests:** The authors declare no competing interests.

**Publisher's note:** Springer Nature remains neutral with regard to jurisdictional claims in published maps and institutional affiliations.



**Open Access** This article is licensed under a Creative Commons Attribution 4.0 International License, which permits use, sharing, adaptation, distribution and reproduction in any medium or format, as long as you give appropriate credit to the original author(s) and the source, provide a link to the Creative Commons license, and indicate if changes were made. The images or other third party material in this article are included in the article's Creative Commons license, unless indicated otherwise in a credit line to the material. If material is not included in the article's Creative Commons license and your intended use is not permitted by statutory regulation or exceeds the permitted use, you will need to obtain permission directly from the copyright holder. To view a copy of this license, visit <http://creativecommons.org/licenses/by/4.0/>.

© The Author(s) 2018